Steel and Composite Structures, *Vol. 27, No. 4 (2018) 465-477*
DOI: https://doi.org/10.12989/scs.2018.27.4.465

Mathematical modeling of smart nanoparticles-reinforced concrete foundations: Vibration analysis

Masood Kargar and Mahmood Rabani Bidgoli *

Department of Civil Engineering, Khomein Branch, Islamic Azad University, Khomein, Iran

(*Received January 7, 2018, Revised March 5, 2018, Accepted March 23, 2018*)

Abstract. In this research, vibration and smart control analysis of a concrete foundation reinforced by SiO_2 nanoparticles and covered by piezoelectric layer on soil medium is investigated. The soil medium is simulated with spring constants and the Mori-Tanaka low is used for obtaining the material properties of nano-composite structure and considering agglomeration effects. With considering first order shear deformation theory, the total potential energy of system is calculated and by means of Hamilton's principle in three displacement directions and electric potential, the six coupled equilibrium equations are obtained. Also, based an analytical method, the frequency of system is calculated. The effects of applied voltage, volume percent and agglomeration of SiO_2 nanoparticles, soil medium and geometrical parameters of structure are shown on the frequency of system. Results show that with applying negative voltage, the frequency of structure is increased.

Keywords: concrete foundation; vibration; piezoelectric layer; soil medium; analytical method

1. Introduction

Various external and internal sources generate vibration instabilities in buildings, such as the motorway traffic, existence of industrial equipment (for instance compressors, crushers, sieve shaker and dryer) or people walking inside the building. These vibrations also affect the performance of concrete foundations and therefore the vibrations may need to be reduced. Vibrations can be reduced by improving the properties of concrete slabs or by using new technologies, such as the use of piezoelectric materials. Concrete foundation can be modified by being mixed with nano material in order to increase its stiffness. In this subject, it can be mentioned a research on reducing building vibrations through foundation improvement by Persson *et al*. (2016).

The vibration behavior of plates on elastic foundations has attracted considerable attention in recent years. Lam *et al*. (2000) used the Green's functions to obtain canonical exact solutions of elastic bending, buckling and vibration for Levy plates resting on two-parameter elastic foundations. Buczkowski and Torbacki (2001) presented a finite element method for the thick plates on two-parameter elastic foundation. By employing the Rayleigh-Ritz method, the three dimensional vibration of rectangular thick plates on elastic foundations was investigated by Zhou *et al*. (2004). The free vibrations of simply supported rectangular plates, resting on two different models of soils, were considered by De Rosa and Lippiello (2009). Ferreira *et al*. (2010) used the radial basis function collocation method to study static deformation and free vibration of plates on Pasternak foundation. Nonlinear vibration analysis of laminated plates resting on nonlinear two-parameters elastic foundations was studied by Akgoz and Civalek (2011). Kumar and Lal (2012) studied the vibration analysis of nonhomogeneous orthotropic rectangular plates with bilinear thickness variation resting on Winkler foundation. Bahmyari and Khedmati (2013) considered the vibration analysis of nonhomogeneous moderately thick plates with point supports resting on Pasternak elastic foundation using element free Galerkin method. Vibrational analysis of advanced composite plates resting on elastic foundation was studied by Mantari *et al*. (2014). They derived the governing equations of a type of functionally graded plates resting on elastic foundation by employing the Hamilton's principal. An original first shear deformation theory to study advanced composites on elastic foundation was presented by Mantari and Granados (2016). Uğurlu (2016) analyzed the vibration of elastic bottom plates of fluid storage tanks resting on Pasternak foundation based on boundary element method. Bounouara *et al*. (2016) investigated a nonlocal zeroth-order shear deformation theory for free vibration of functionally graded nanoscale plates resting on elastic foundation. Also, a dimensionless parametric study for forced vibrations of foundation-soil systems was done by Chen *et al*. (2016a). A non-polynomial four variable refined plate theory for free vibration of functionally graded thick rectangular plates on elastic foundation was investigated by Meftah *et al*. (2017).

None of the above researchers have considered piezo-based nano-composite structures. Mechanical analysis of nanostructures has been reported by many researchers (Zemri *et al*. 2015, Larbi Chaht *et al*. 2015, Belkorissat *et al*. 2015, Ahouel *et al*. 2016, Bounouara *et al*. 2016, Bouafia *et al*. 2017, Besseghier *et al*. 2017, Bellifa *et al*. 2017, Mouffoki *et al*. 2017, Khetir *et al*. 2017). In recent

*Corresponding author, Ph.D., Assistant Professor,
E-mail: m.rabanibidgoli@gmail.com

Copyright © 2018 Techno-Press, Ltd.

ISSN: 1229-9367 (Print), 1598-6233 (Online)

years, theoretical and experimental studies have been conducted on nano-composites subjected to electric field. Static analysis of FG-CNT reinforced composite plate imbedded in piezoelectric layers with three cases of CNT distribution based on three-dimensional theory was discussed by Alibeigloo (2013). Piezo-based wireless sensor network for early-age concrete strength monitoring is planned by Chen *et al*. (2016b). Van Thu and Duc (2016) presented an analytical approach to investigate the non-linear dynamic response and vibration of an imperfect three-phase laminated nanocomposite cylindrical panel resting on elastic foundations in thermal environments. Sasmal *et al*. (2017) investigated electrical conductivity and piezo-resistive characteristics of CNT and CNF incorporated cementitious nanocomposites under static and dynamic loading. In magneto-electro-elastic (MEE) composite materials a coupling between mechanical, electric and magnetic fields results in the ability to exchange energy among these three energy forms. These materials have direct application in sensors and actuators, damping and control of vibrations in structures. Xue *et al*. (2011) studied the large deflection of a rectangular MEE thin plate for the first time based on the classical plate theory. Li and Zhang (2014) investigated the free vibration of a MEE plate resting on a Pasternak foundation by using the Mindlin theory. Large amplitude free vibration of symmetrically laminated magneto-electro-elastic rectangular plates on Pasternak type foundation was investigated by Shooshtari and Razavi (2015). Ebrahimi *et al*. (2017) proposed a four-variable shear deformation refined plate theory for free vibration analysis of embedded smart plates made of porous magneto-electro-elastic functionally graded (MEE-FG) materials resting on elastic foundations. Duc *et al*. (2017a, b, c) studied thermal and mechanical stability of a functionally graded composite truncated conical shell, plates and double curved shallow shells reinforced by carbon nanotube fibers. Based on Reddy's third-order shear deformation plate theory, the nonlinear dynamic response and vibration of imperfect functionally graded carbon nanotube-reinforced composite plates was analyzed by Thanh *et al*. (2017). Duc *et al*. (2018) presented the first analytical approach to investigate the nonlinear dynamic response and vibration of imperfect rectangular nanocompsite multilayer organic solar cell subjected to mechanical loads using the classical plate theory.

Furthermore, the mechanical behavior of concrete structures containing nanoparticles has been investigated experimentally by a number of researchers, but there is little mathematical control in this field. Nirmala and Dhanalakshmi (2015) studied the Influence of nano materials in the distressed retaining structure for crack filling. The influences of nanoparticles on dynamic strength of ultra-high performance concrete was tested by Su *et al*. (2016). Fathi *et al*. (2017) investigated the Mechanical and physical properties of expanded polystyrene structural concretes containing Micro-silica and Nano-silica. In the field of mathematical modeling of concrete structures, Jafarian Arani and Kolahchi (2016) studied the buckling analysis of concrete columns reinforced with carbon nanotubes by using Euler-Bernoulli and Timoshenko beam models. Zamanian *et al*. (2017) investigated the nonlinear buckling of a concrete column reinforced with SiO_2 nanoparticles. Also, Arbabi *et al*. (2017) explored the buckling of concrete columns reinforced with Zinc Oxide nanoparticles subjected to electric field.

To the best of the authors' knowledge, the effects of using nano particles and piezoelectric layer on the vibration of concrete foundations have not been investigated. So, this study is done to fill the gap in this area. The purpose of this paper is to study the free vibration smart control of concrete foundation reinforced by SiO_2 nanoparticles embedded in soli medium. The structure is covered by a piezoelectric layer subjected to external voltage. In order to obtain the equivalent material properties of nanocomposite structure, the Mori-Tanaka model is used. Applying first order shear deformation theory (FSDT), the motion equations are achieved based on Hamilton's principal. Navier method is applied for obtaining the frequency of the system. The effects of applied voltage, volume percent and agglomeration of SiO_2 nanoparticles, soil medium and geometrical parameters of structure on the frequency of system are disused in detail.

2. Mathematical model

As shown in Fig. 1, a concrete foundation reinforced with SiO_2 nanoparticles and covered by piezoelectric layer with length L, width b, concrete thickness h and piezoelectric layer thickness hp is considered.

2.1 FSDT theory

There are many new theories for modeling of different structures. Some of the new theories have been used by Tounsi and co-authors (Bessaim *et al*. 2013, Bouderba *et al*. 2013, 2016, Belabed *et al*. 2014, Zidi *et al*. 2014, Bourada *et al*. 2015, Bousahla *et al*. 2016, Beldjelili *et al*. 2016, Boukhari *et al*. 2016, Draiche *et al*. 2016, Attia *et al*. 2015, Mahi *et al*. 2015, Bennoun *et al*. 2016, El-Haina *et al*. 2017, Menasria *et al*. 2017, Chikh *et al*. 2017, Henderson *et al*. 2018, Sanada 2018, Stelson 2018).

Based on FSDT shell theory, the displacement field can be expressed as (Reddy 2002)

$$u(x,\theta,z,t)=u(x,\theta,t)+z\phi_x(x,\theta,t), \tag{1a}$$

$$v(x,\theta,z,t)=v(x,\theta,t)+z\phi_\theta(x,\theta,t), \tag{1b}$$

$$w(x,\theta,z,t)=w(x,\theta,t), \tag{1c}$$

where (u (x, θ, z, t), v(x, θ, z, t), w(x, θ, z, t)) denote the displacement components at an arbitrary point (x, θ, z) in the shell, and (u (x, θ, t), v(x, θ, t), w(x, θ, t)) are the displacement of a material point at (x, θ) on the mid-plane (i.e., z = 0) of the shell along the x-, θ-, and z-directions, respectively; ϕ_x and ϕ_θ are the rotations of the normal to the mid-plane about x- and θ- directions, respectively. Based on

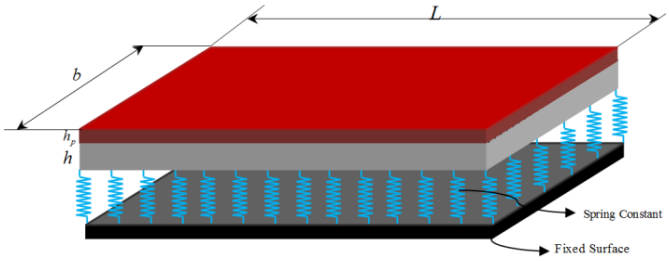

Fig. 1 A schematic figure for concrete foundation with piezoelectric layers reinforced with SiO_2 nanoparticles

above relations, the strain-displacement equations may be written as

$$\varepsilon_{xx}=\frac{\partial u}{\partial x}+z\frac{\partial \phi_x}{\partial x}, \tag{2a}$$

$$\varepsilon_{\theta\theta}=\frac{1}{R}\left(w+\frac{\partial v}{\partial \theta}\right)+\frac{z}{R}\frac{\partial \phi_\theta}{\partial \theta}, \tag{2b}$$

$$\gamma_{x\theta}=\frac{\partial v}{\partial x}+\frac{1}{R}\left(\frac{\partial u}{\partial \theta}\right)+z\left(\frac{\partial \phi_\theta}{\partial x}+\frac{1}{R}\frac{\partial \phi_x}{\partial \theta}\right), \tag{2c}$$

$$\gamma_{xz}=\phi_x+\frac{\partial w}{\partial x}, \tag{2d}$$

$$\gamma_{z\theta}=\frac{1}{R}\left(\frac{\partial w}{\partial \theta}-v\right)+\phi_\theta. \tag{2e}$$

where (ε_{xx}, $\varepsilon_{\theta\theta}$) are the normal strain components and ($\gamma_{\theta z}$, γ_{xz}, $\gamma_{x\theta}$) are the shear strain components.

2.2 Constitutive equations of piezoelectric material

In a piezoelectric material, application of an electric field to it will cause a strain proportional to the mechanical field strength, and vice versa. The constitutive equation for stresses σ and strains ε matrix on the mechanical side, as well as flux density D and field strength E matrix on the electrostatic side, may be arbitrarily combined as follows (Kolahchi *et al*. 2016)

$$\begin{bmatrix}\sigma_{xx}\\ \sigma_{yy}\\ \sigma_{zz}\\ \tau_{yz}\\ \tau_{xz}\\ \tau_{xy}\end{bmatrix}=\begin{bmatrix}C_{11}&C_{12}&C_{13}&0&0&0\\ C_{12}&C_{22}&C_{23}&0&0&0\\ C_{13}&C_{23}&C_{33}&0&0&0\\ 0&0&0&C_{44}&0&0\\ 0&0&0&0&C_{55}&0\\ 0&0&0&0&0&C_{66}\end{bmatrix}\left(\begin{Bmatrix}\varepsilon_{xx}\\ \varepsilon_{yy}\\ \varepsilon_{zz}\\ \gamma_{yz}\\ \gamma_{xz}\\ \gamma_{xy}\end{Bmatrix}\right)-\begin{bmatrix}0&0&e_{31}\\ 0&0&e_{32}\\ 0&0&e_{33}\\ 0&e_{24}&0\\ e_{15}&0&0\\ 0&0&0\end{bmatrix}\begin{Bmatrix}E_x\\ E_y\\ E_z\end{Bmatrix} \tag{3}$$

$$\begin{bmatrix}D_x\\ D_y\\ D_z\end{bmatrix}=\begin{bmatrix}0&0&0&0&e_{15}&0\\ 0&0&0&e_{24}&0&0\\ e_{31}&e_{31}&e_{33}&0&0&0\end{bmatrix}\left(\begin{Bmatrix}\varepsilon_{xx}\\ \varepsilon_{yy}\\ \varepsilon_{zz}\\ \gamma_{yz}\\ \gamma_{xz}\\ \gamma_{xy}\end{Bmatrix}\right)+\begin{bmatrix}\in_{11}&0&0\\ 0&\in_{22}&0\\ 0&0&\in_{33}\end{bmatrix}\begin{Bmatrix}E_x\\ E_y\\ E_z\end{Bmatrix} \tag{4}$$

where σ_{ij}, ε_{ij}, D_{ii} and E_{ii} are stress, strain, electric displacement and electric field, respectively. Also, C_{ij}, e_{ij} and $\in_{ij}$ denote elastic, piezoelectric and dielectric coefficients, respectively. Noted that C_{ij} and α_{xx}, $\alpha_{\theta\theta}$ may be obtained using Mori-Tanaka model (Mori and Tanaka 1973). The electric field in terms of electric potential (Φ) is expressed as

$$E_k=-\nabla\Phi, \tag{5}$$

where, the electric potential is assumed as the combination of a half-cosine and linear variation, which satisfies the Maxwell equation. It can be written as (Kolahchi *et al*. 2016)

$$\Phi(x,y,z,t)=-\cos(\frac{\pi z}{h})\varphi(x,y,t)+\frac{2V_0 z}{h}, \tag{6}$$

where ϕ (x, θ, t) is the time and spatial distribution of the electric potential which must satisfy the electric boundary conditions, V_0 is external electric voltage.

However, using Eq. (1), the governing equations of piezoelectric material (i.e., Eqs. (3) and (4)) for FSDT may be written as

$$\sigma_{xx}^{p}=C_{11}\varepsilon_{xx}+C_{12}\varepsilon_{yy}+e_{31}\left(\frac{\pi}{h}\sin\left(\frac{\pi z}{h}\right)\varphi+\frac{2V_0}{h}\right), \tag{7}$$

$$\sigma_{yy}^{p}=C_{12}\varepsilon_{xx}+C_{22}\varepsilon_{yy}+e_{32}\left(\frac{\pi}{h}\sin\left(\frac{\pi z}{h}\right)\varphi+\frac{2V_0}{h}\right), \tag{8}$$

$$\tau_{yz}^{p}=C_{44}\gamma_{yz}-e_{15}\left(\cos\left(\frac{\pi z}{h}\right)\frac{\partial\varphi}{\partial y}\right), \tag{9}$$

$$\tau_{xz}^{p}=C_{55}\gamma_{zx}-e_{24}\left(\cos\left(\frac{\pi z}{h}\right)\frac{\partial\varphi}{\partial x}\right), \tag{10}$$

$$\tau_{xy}^{p}=C_{66}\gamma_{xy}, \tag{11}$$

$$D_x=e_{15}\gamma_{xz}+\in_{11}\left(\cos\left(\frac{\pi z}{h}\right)\frac{\partial\varphi}{\partial y}\right), \tag{12}$$

$$D_y=e_{24}\gamma_{zy}+\in_{22}\left(\cos\left(\frac{\pi z}{h}\right)\frac{\partial\varphi}{\partial y}\right), \tag{13}$$

$$D_x = e_{31}\varepsilon_{xx} + e_{32}\varepsilon_{yy} - \in_{33}\left(\frac{\pi}{h}\sin\left(\frac{\pi z}{h}\right)\varphi + \frac{2V_0}{h}\right). \quad (14)$$

For the concrete foundation, with neglecting the piezoelectric properties we have

$$\sigma_{xx}^c = Q_{11}\varepsilon_{xx} + Q_{12}\varepsilon_{yy}, \quad (15)$$

$$\sigma_{yy}^c = Q_{12}\varepsilon_{xx} + Q_{22}\varepsilon_{yy}, \quad (16)$$

$$\tau_{yz}^c = Q_{44}\gamma_{yz}, \quad (17)$$

$$\tau_{xz}^c = Q_{55}\gamma_{zx}, \quad (18)$$

$$\tau_{xy}^c = Q_{66}\gamma_{xy}, \quad (19)$$

2.3 Mori-Tanaka Model and agglomeration effects

In this section, the effective modulus of the concrete foundation reinforced by SiO_2 nanoparticles is developed. Different methods are available to obtain the average properties of a composite. Due to its simplicity and accuracy even at high volume fractions of the inclusions, the Mori-Tanaka method is employed in this section. The matrix is assumed to be isotropic and elastic, with the Young's modulus E_m and the Poisson's ratio υ_m. The constitutive relations for a layer of the composite with the principal axes parallel to the r, θ and z directions are (Mori and Tanaka 1973)

$$\begin{Bmatrix}\sigma_{11}\\ \sigma_{22}\\ \sigma_{33}\\ \sigma_{23}\\ \sigma_{13}\\ \sigma_{12}\end{Bmatrix} = \begin{bmatrix} k+m & l & k-m & 0 & 0 & 0\\ l & n & l & 0 & 0 & 0\\ k-m & l & k+m & 0 & 0 & 0\\ 0 & 0 & 0 & p & 0 & 0\\ 0 & 0 & 0 & 0 & m & 0\\ 0 & 0 & 0 & 0 & 0 & p \end{bmatrix}\begin{Bmatrix}\varepsilon_{11}\\ \varepsilon_{22}\\ \varepsilon_{33}\\ \gamma_{23}\\ \gamma_{13}\\ \gamma_{12}\end{Bmatrix} \quad (20)$$

where σ_{ij}, ε_{ij}, $\gamma_{\theta z}$, k, m, n, l, p are the stress components, the strain components and the stiffness coefficients respectively. According to the Mori-Tanaka method the stiffness coefficients are given by

$$\begin{aligned}
k &= \frac{E_m\{E_m c_m + 2k_r(1+\nu_m)[1+c_r(1-2\nu_m)]\}}{2(1+\nu_m)[E_m(1+c_r-2\nu_m)+2c_m k_r(1-\nu_m-2\nu_m^2)]}\\
l &= \frac{E_m\{c_m\nu_m[E_m+2k_r(1+\nu_m)]+2c_r l_r(1-\nu_m^2)]\}}{(1+\nu_m)[E_m(1+c_r-2\nu_m)+2c_m k_r(1-\nu_m-2\nu_m^2)]}\\
n &= \frac{E_m^2 c_m(1+c_r-c_m\nu_m)+2c_m c_r(k_r n_r - l_r^2)(1+\nu_m)^2(1-2\nu_m)}{(1+\nu_m)[E_m(1+c_r-2\nu_m)+2c_m k_r(1-\nu_m-2\nu_m^2)]}\\
&\quad + \frac{E_m[2c_m^2 k_r(1-\nu_m)+c_r n_r(1+c_r-2\nu_m)-4c_m l_r\nu_m]}{E_m(1+c_r-2\nu_m)+2c_m k_r(1-\nu_m-2\nu_m^2)}\\
p &= \frac{E_m[E_m c_m + 2p_r(1+\nu_m)(1+c_r)]}{2(1+\nu_m)[E_m(1+c_r)+2c_m p_r(1+\nu_m)]}\\
m &= \frac{E_m[E_m c_m + 2m_r(1+\nu_m)(3+c_r-4\nu_m)]}{2(1+\nu_m)\{E_m[c_m+4c_r(1-\nu_m)]+2c_m m_r(3-\nu_m-4\nu_m^2)\}}
\end{aligned} \quad (21)$$

where the subscripts m and r stand for matrix and reinforcement respectively. C_m and C_r are the volume fractions of the matrix and the nanoparticles respectively and k_r, l_r, n_r, p_r, m_r are the Hills elastic modulus for the nanoparticles (Mori and Tanaka 1973). The experimental results show that the assumption of uniform dispersion for nanoparticles in the matrix is not correct and the most of nanoparticles are bent and centralized in one area of the matrix. These regions with concentrated nanoparticles are assumed to have spherical shapes, and are considered as ''inclusions'' with different elastic properties from the surrounding material. The total volume V_r of nanoparticles can be divided into the following two parts (Shi and Feng 2004)

$$V_r = V_r^{inclusion} + V_r^m \quad (22)$$

where $V_r^{inclusion}$ and V_r^m are the volumes of nanoparticles dispersed in the spherical inclusions and in the matrix, respectively. Introduce two parameters ξ and ζ describe the agglomeration of nanoparticles

$$\xi = \frac{V_{inclusion}}{V}, \quad (23)$$

$$\zeta = \frac{V_r^{inclusion}}{V_r}. \quad (24)$$

However, the average volume fraction c_r of nanoparticles in the composite is

$$C_r = \frac{V_r}{V}. \quad (25)$$

Assume that all the orientations of the nanoparticles are completely random. Hence, the effective bulk modulus (K) and effective shear modulus (G) may be written as

$$K = K_{out}\left[1 + \frac{\xi\left(\frac{K_{in}}{K_{out}}-1\right)}{1+\alpha(1-\xi)\left(\frac{K_{in}}{K_{out}}-1\right)}\right], \quad (26)$$

$$G = G_{out}\left[1 + \frac{\xi\left(\frac{G_{in}}{G_{out}}-1\right)}{1+\beta(1-\xi)\left(\frac{G_{in}}{G_{out}}-1\right)}\right], \quad (27)$$

where

$$K_{in} = K_m + \frac{(\delta_r - 3K_m\chi_r)C_r\zeta}{3(\xi - C_r\zeta + C_r\zeta\chi_r)}, \quad (28)$$

$$K_{out} = K_m + \frac{C_r(\delta_r - 3K_m\chi_r)(1-\zeta)}{3\left[1-\xi-C_r(1-\zeta)+C_r\chi_r(1-\zeta)\right]}, \quad (29)$$

$$G_{in} = G_m + \frac{(\eta_r - 3G_m\beta_r)C_r\zeta}{2(\xi - C_r\zeta + C_r\zeta\beta_r)}, \quad (30)$$

$$G_{out}=G_m+\frac{C_r\left(\eta_r-3G_m\beta_r\right)\left(1-\zeta\right)}{2\left[1-\xi-C_r\left(1-\zeta\right)+C_r\beta_r\left(1-\zeta\right)\right]}, \quad (31)$$

where χ_r, β_r, δ_r, η_r may be calculated as

$$\chi_r=\frac{3\left(K_m+G_m\right)+k_r-l_r}{3\left(k_r+G_m\right)}, \quad (32)$$

$$\beta_r=\frac{1}{5}\left\{\begin{array}{l}\dfrac{4G_m+2k_r+l_r}{3\left(k_r+G_m\right)}+\dfrac{4G_m}{\left(p_r+G_m\right)}\\ +\dfrac{2\left[G_m\left(3K_m+G_m\right)+G_m\left(3K_m+7G_m\right)\right]}{G_m\left(3K_m+G_m\right)+m_r\left(3K_m+7G_m\right)}\end{array}\right\}, \quad (33)$$

$$\delta_r=\frac{1}{3}\left[n_r+2l_r+\frac{\left(2k_r-l_r\right)\left(3K_m+2G_m-l_r\right)}{k_r+G_m}\right], \quad (34)$$

$$\begin{aligned}\eta_r=\frac{1}{5}\Bigg[&\frac{2}{3}\left(n_r-l_r\right)+\frac{4G_m p_r}{\left(p_r+G_m\right)}\\&+\frac{8G_m m_r\left(3K_m+4G_m\right)}{3K_m\left(m_r+G_m\right)+G_m\left(7m_r+G_m\right)}\\&+\frac{2\left(k_r-l_r\right)\left(2G_m+l_r\right)}{3\left(k_r+G_m\right)}\Bigg].\end{aligned} \quad (35)$$

where, K_m and G_m are the bulk and shear moduli of the matrix which can be written as

$$K_m=\frac{E_m}{3\left(1-2\upsilon_m\right)}, \quad (36)$$

$$G_m=\frac{E_m}{2\left(1+\upsilon_m\right)}. \quad (37)$$

Furthermore, β, α can be obtained from

$$\alpha=\frac{\left(1+\upsilon_{out}\right)}{3\left(1-\upsilon_{out}\right)}, \quad (38)$$

$$\beta=\frac{2\left(4-5\upsilon_{out}\right)}{15\left(1-\upsilon_{out}\right)}, \quad (39)$$

$$\upsilon_{out}=\frac{3K_{out}-2G_{out}}{6K_{out}+2G_{out}}. \quad (40)$$

Finally, the elastic modulus (E) and poison's ratio (υ) can be calculated as

$$E=\frac{9KG}{3K+G}, \quad (41)$$

$$\upsilon=\frac{3K-2G}{6K+2G}. \quad (42)$$

2.4 Energy method

The total potential energy, V, of the system is the sum of potential energy, U, kinetic energy, K, and the work done by the elastic medium, W.

2.4.1 Potential energy

The potential energy can be written as

$$U=\frac{1}{2}\int\left(\begin{array}{l}\sigma_{xx}^c\varepsilon_{xx}+\sigma_{yy}^c\varepsilon_{yy}+\tau_{xz}^c\gamma_{xz}+\tau_{yz}^c\gamma_{yz}+\tau_{xy}^c\gamma_{xy}\\+\sigma_{xx}^p\varepsilon_{xx}+\sigma_{yy}^p\varepsilon_{yy}+\tau_{xz}^p\gamma_{xz}+\tau_{yz}^p\gamma_{yz}+\tau_{xy}^p\gamma_{xy}\\-D_xE_x-D_yE_y-D_zE_z\end{array}\right)dV, \quad (43)$$

Combining of Eqs. (1), (7)-(14) and (43) yields

$$\begin{aligned}U=\frac{1}{2}\int_0^{2\pi}\int_0^L\Bigg\{&\left[N_{xx}\frac{\partial u}{\partial x}+M_{xx}\frac{\partial\phi_x}{\partial x}\right]\\&+\left[N_{yy}\frac{\partial v}{\partial y}+M_{yy}\frac{\partial\phi_y}{\partial y}\right]+Q_x\left(\phi_x+\frac{\partial w}{\partial x}\right)\\&+N_{xy}\left[\frac{\partial v}{\partial x}+\frac{\partial u}{\partial y}\right]+M_{xy}\left[\frac{\partial\phi_y}{\partial x}+\frac{\partial\phi_x}{\partial y}\right]Rxdy\\&+Q_y\left[\frac{\partial w}{\partial y}+\phi_y\right]+\int_{-h/2}^{h/2+h_p}\int_0^{2\pi}\int_0^L-\\&-D_x\left[\cos\left(\frac{\pi z}{h}\right)\frac{\partial\varphi}{\partial x}\right]-D_\theta\left[\cos\left(\frac{\pi z}{h}\right)\frac{\partial\varphi}{\partial y}\right]\\&-D_z\left[-\frac{\pi}{h}\sin\left(\frac{\pi z}{h}\right)\varphi-\frac{2V_0}{h}\right]\Bigg\}dxdydz,\end{aligned} \quad (44)$$

where the stress resultant-displacement relations can be written as

$$\left\{\begin{array}{l}N_{xx}\\N_{yy}\\N_{xy}\end{array}\right\}=\int_{-\frac{h}{2}}^{\frac{h}{2}}\left\{\begin{array}{l}\sigma_{xx}^c\\\sigma_{yy}^c\\\tau_{xy}^c\end{array}\right\}dz+\int_{\frac{h}{2}}^{\frac{h}{2}+h_p}\left\{\begin{array}{l}\sigma_{xx}^p\\\sigma_{yy}^p\\\tau_{xy}^p\end{array}\right\}dz \quad (45)$$

$$\left\{\begin{array}{l}Q_x\\Q_\theta\end{array}\right\}=k'\int_{-\frac{h}{2}}^{\frac{h}{2}}\left\{\begin{array}{l}\tau_{xz}^c\\\tau_{yz}^c\end{array}\right\}dz+k'\int_{-\frac{h}{2}}^{\frac{h}{2}+h_p}\left\{\begin{array}{l}\tau_{xz}^p\\\tau_{yz}^p\end{array}\right\}dz, \quad (46)$$

$$\left\{\begin{array}{l}M_{xx}\\M_{yy}\\M_{xy}\end{array}\right\}=\int_{-\frac{h}{2}}^{\frac{h}{2}}\left\{\begin{array}{l}\sigma_{xx}^c\\\sigma_{yy}^c\\\tau_{xy}^c\end{array}\right\}z\,dz+\int_{\frac{h}{2}}^{\frac{h}{2}+h_p}\left\{\begin{array}{l}\sigma_{xx}^p\\\sigma_{yy}^p\\\tau_{xy}^p\end{array}\right\}z\,dz, \quad (47)$$

In which k' is shear correction coefficient. Substituting Eqs. (1) and (7)-(14) into Eqs. (45)-(47), the stress resultant-displacement relations can be obtained as follow

$$N_{xx}=A_{110}\frac{\partial u}{\partial x}+A_{111}\frac{\partial\phi_x}{\partial x}+A_{120}\frac{\partial v}{\partial y}+A_{121}\frac{\partial\phi_y}{\partial y}+E_{31}\varphi, \quad (48)$$

$$N_{yy} = A_{120}\frac{\partial u}{\partial x} + A_{121}\frac{\partial \phi_x}{\partial x} + A_{220}\frac{\partial v}{\partial y} + A_{221}\frac{\partial \phi_y}{\partial y} + E_{32}\varphi, \quad (49)$$

$$Q_y = k' A_{44}\left[\frac{\partial w}{\partial y} + \phi_y\right] + E_{15}\frac{\partial \varphi}{\partial y}, \quad (50)$$

$$Q_x = k' A_{55}\left(\frac{\partial w}{\partial x} + \phi_x\right) + E_{24}\frac{\partial \varphi}{\partial x}, \quad (51)$$

$$N_{xy} = A_{660}\left(\frac{\partial u}{\partial y} + \frac{\partial v}{\partial x}\right) + A_{661}\left(\frac{\partial \phi_x}{\partial y} + \frac{\partial \phi_y}{\partial x}\right), \quad (52)$$

$$M_{xx} = A_{111}\frac{\partial u}{\partial x} + A_{112}\frac{\partial \phi_x}{\partial x} + A_{121}\frac{\partial v}{\partial y} + A_{122}\frac{\partial \phi_y}{\partial y} + F_{31}\varphi, \quad (53)$$

$$M_{yy} = A_{121}\frac{\partial u}{\partial x} + A_{122}\frac{\partial \phi_x}{\partial x} + A_{221}\frac{\partial v}{\partial y} + A_{222}\frac{\partial \phi_y}{\partial y} + F_{32}\varphi, \quad (54)$$

$$M_{xy} = A_{661}\left(\frac{\partial u}{\partial y} + \frac{\partial v}{\partial x}\right) + A_{662}\left(\frac{\partial \phi_x}{\partial y} + \frac{\partial \phi_\theta}{\partial x}\right), \quad (55)$$

Where

$$A_{11k} = \int_{-h/2}^{h/2} Q_{11} z^k dz + \int_{-h/2}^{h/2+h_p} C_{11} z^k dz, \quad k = 0, 1, 2 \quad (56)$$

$$A_{12k} = \int_{-h/2}^{h/2} Q_{12} z^k dz + \int_{-h/2}^{h/2+h_p} C_{12} z^k dz, \quad k = 0, 1, 2 \quad (57)$$

$$A_{22k} = \int_{-h/2}^{h/2} Q_{22} z^k dz + \int_{-h/2}^{h/2+h_p} C_{22} z^k dz, \quad k = 0, 1, 2 \quad (58)$$

$$A_{66k} = \int_{-h/2}^{h/2} Q_{66} z^k dz + \int_{-h/2}^{h/2+h_p} C_{66} z^k dz, \quad k = 0, 1, 2 \quad (59)$$

$$A_{44} = \int_{-h/2}^{h/2} Q_{44} dz + \int_{-h/2}^{h/2+h_p} C_{44} dz, \quad (60)$$

$$A_{55} = \int_{-h/2}^{h/2} Q_{55} dz + \int_{-h/2}^{h/2+h_p} C_{55} dz, \quad (61)$$

$$(E_{31}, E_{32}) = \frac{\pi}{h}\int_{-h/2}^{h/2} (e_{31}, e_{32}) \sin\left(\frac{\pi z}{h}\right) dz, \quad (62)$$

$$(E_{24}, E_{15}) = -\int_{-h/2}^{h/2} (e_{24}, e_{15}) \cos\left(\frac{\pi z}{h}\right) dz, \quad (63)$$

$$(F_{31}, F_{32}) = \frac{\pi}{h}\int_{-h/2}^{h/2} (e_{31}, e_{32}) \sin\left(\frac{\pi z}{h}\right) z dz, \quad (64)$$

2.4.2 Kinetic energy

The kinetic energy of system may be written as

$$K = \frac{(\rho^c + \rho^p)}{2}\int \left(\left(\frac{\partial u}{\partial t} + z\frac{\partial \phi_x}{\partial t}\right)^2 + \left(\frac{\partial v}{\partial t} + z\frac{\partial \phi_y}{\partial t}\right)^2 + \left(\frac{\partial w}{\partial t}\right)^2\right) dV. \quad (65)$$

Defining the moments of inertia as below

$$\begin{Bmatrix} I_0 \\ I_1 \\ I_2 \end{Bmatrix} = \int_{-h/2}^{h/2} \begin{bmatrix} \rho^c \\ \rho^c z \\ \rho^c z^2 \end{bmatrix} dz + \int_{h/2}^{h/2+h_p} \begin{bmatrix} \rho^p \\ \rho^p z \\ \rho^p z^2 \end{bmatrix} dz, \quad (66)$$

the kinetic energy may be written as

$$K = \frac{1}{2}\int \left(I_0\left(\left(\frac{\partial u}{\partial t}\right)^2 + \left(\frac{\partial v}{\partial t}\right)^2 + \left(\frac{\partial w}{\partial t}\right)^2\right) + I_1\left(2\frac{\partial u}{\partial t}\frac{\partial \phi_x}{\partial t} + 2\frac{\partial v}{\partial t}\frac{\partial \phi_y}{\partial t}\right) + I_2\left(\left(\frac{\partial \phi_x}{\partial t}\right)^2 + \left(\frac{\partial \phi_y}{\partial t}\right)^2\right) dA, \quad (67)$$

2.4.3 External works

The external work due to soil medium can be written as (Bowles 1988)

$$W_e = \int_0^{2\pi}\int_0^L (-K_w w) dx dy, \quad (68)$$

where K_w is Winkler's spring modulus. In addition, the in-plane forces may be written as

$$W_f = -\frac{1}{2}\int \left[N_{xx}^f \left(\frac{\partial w}{\partial x}\right)^2 + N_{yy}^f \left(\frac{\partial w}{\partial y}\right)^2\right] dx dy. \quad (69)$$

where

$$N_{xx}^f = N_{xx}^M + N_{xx}^E = N_{xx}^M + 2V_0 e_{31}, \quad (70)$$

$$N_{yy}^f = N_{yy}^M + N_{yy}^E = N_{yy}^M + 2V_0 e_{32}. \quad (71)$$

2.5 Motion equations

The governing equations can be derived by Hamilton's principal as follows

$$\int_0^t (\delta U - \delta K - \delta W_e - \delta W_f) dt = 0. \quad (72)$$

Substituting Eqs. (42), (67), (68) and (71) into Eq. (72) yields the following governing equations

$$\delta u: \frac{\partial N_{xx}}{\partial x} + \frac{\partial N_{xy}}{\partial y} = I_0\frac{\partial^2 u}{\partial t^2} + I_1\frac{\partial^2 \phi_x}{\partial t^2}, \quad (73)$$

$$\delta v: \frac{\partial N_{xy}}{\partial x} + \frac{\partial N_{yy}}{\partial y} = I_0\frac{\partial^2 v}{\partial t^2} + I_1\frac{\partial^2 \phi_y}{\partial t^2}, \quad (74)$$

$$\delta w: \frac{\partial Q_x}{\partial x} + \frac{\partial Q_y}{\partial y} + N_{xx}^f\frac{\partial^2 w}{\partial x^2} + N_{yy}^f\frac{\partial^2 w}{\partial y^2} - K_w w = I_0\frac{\partial^2 w}{\partial t^2}, \quad (75)$$

$$\delta\phi_x : \frac{\partial M_{xx}}{\partial x}+\frac{\partial M_{xy}}{\partial y}-Q_x = I_2\frac{\partial^2\phi_x}{\partial t^2}+I_1\frac{\partial^2 u}{\partial t^2}, \tag{76}$$

$$\delta\varphi_y : \frac{\partial M_{xy}}{\partial x}+\frac{\partial M_{xx}}{\partial y}-Q_y = I_2\frac{\partial^2\phi_y}{\partial t^2}+I_1\frac{\partial^2 v}{\partial t^2}, \tag{77}$$

$$\begin{aligned}\delta\varphi: \int_{-h/2}^{h/2}\Bigg\{&\left[\cos\left(\frac{\pi z}{h}\right)\frac{\partial D_x}{\partial x}\right]+\left[\cos\left(\frac{\pi z}{h}\right)\frac{\partial D_y}{\partial y}\right]\\&+D_z\left[\frac{\pi}{h}\sin\left(\frac{\pi z}{h}\right)\right]\Bigg\}dz=0\end{aligned} \tag{78}$$

Substituting Eqs. (48) to (55) into Eqs. (73) to (78), the governing equations can be written as follow

$$\begin{aligned}&A_{110}\frac{\partial^2 u}{\partial x^2}+A_{111}\frac{\partial^2\phi_x}{\partial x^2}+A_{120}\frac{\partial^2 v}{\partial y\,\partial x}+A_{121}\frac{\partial^2\phi_y}{\partial y\,\partial x}\\&+E_{31}\frac{\partial\varphi}{\partial x}+A_{120}\frac{\partial^2 u}{\partial x\,\partial y}+A_{121}\frac{\partial^2\phi_x}{\partial x\,\partial y}+A_{220}\frac{\partial^2 v}{\partial y^2}\\&+A_{221}\frac{\partial^2\phi_y}{\partial y^2}+E_{32}\frac{\partial\varphi}{\partial y}=I_0\frac{\partial^2 u}{\partial t^2}+I_1\frac{\partial^2\phi_x}{\partial t^2},\end{aligned} \tag{79}$$

$$\begin{aligned}&A_{120}\frac{\partial^2 u}{\partial x\,\partial y}+A_{121}\frac{\partial^2\phi_x}{\partial x\,\partial y}+A_{220}\frac{\partial^2 v}{\partial y^2}+A_{221}\frac{\partial^2\phi}{\partial y^2}\\&+E_{32}\frac{\partial\varphi}{\partial y}+A_{660}\left(\frac{\partial^2 u}{\partial y\,\partial x}+\frac{\partial^2 v}{\partial x^2}\right)+A_{661}\left(\frac{\partial^2\phi_x}{\partial y\,\partial x}+\frac{\partial^2\phi_y}{\partial x^2}\right)\\&=I_0\frac{\partial^2 v}{\partial t^2}+I_1\frac{\partial^2\phi_y}{\partial t^2},\end{aligned} \tag{80}$$

$$\begin{aligned}&k'A_{44}\left[\frac{\partial w}{\partial y^2}+\frac{\partial\phi_y}{\partial y}\right]+E_{15}\frac{\partial\varphi}{\partial y^2}+k'A_{55}\left(\frac{\partial^2 w}{\partial x^2}+\frac{\partial\phi_x}{\partial x}\right)\\&+E_{24}\frac{\partial^2\varphi}{\partial x^2}-A_{120}\frac{\partial u}{\partial x}-A_{121}\frac{\partial\phi_x}{\partial x}-A_{220}\left(\frac{\partial v}{\partial y}\right)-A_{221}\frac{\partial\phi}{\partial y},\\&N^f_{xx}\frac{\partial^2 w}{\partial x^2}+N^f_{yy}\frac{\partial^2 w}{\partial y^2}-K_w w=I_0\frac{\partial^2 w}{\partial t^2},\end{aligned} \tag{81}$$

$$\begin{aligned}&A_{111}\frac{\partial^2 u}{\partial x^2}+A_{112}\frac{\partial^2\phi_x}{\partial x^2}+A_{121}\left(\frac{\partial^2 v}{\partial y\,\partial x}+\frac{\partial w}{\partial x}\right)+A_{122}\frac{\partial^2\phi_y}{\partial y}+F_{31}\frac{\partial\phi}{\partial x}\\&+A_{661}\left(\frac{\partial^2 u}{\partial y^2}+\frac{\partial^2 v}{\partial x\,\partial y}\right)+A_{662}\left(\frac{\partial^2\phi_x}{\partial y^2}+\frac{\partial^2\phi_y}{\partial x\,\partial y}\right)-k'A_{55}\left(\frac{\partial w}{\partial x}+\phi_x\right)\\&-E_{24}\frac{\partial\varphi}{\partial x}=I_2\frac{\partial^2\phi_x}{\partial t^2}+I_1\frac{\partial^2 u}{\partial t^2},\end{aligned} \tag{82}$$

$$\begin{aligned}&A_{121}\frac{\partial^2 u}{\partial x\,\partial y}+A_{122}\frac{\partial^2\phi_x}{\partial x\,\partial y}+A_{221}\left(\frac{\partial^2 v}{\partial y^2}+\frac{\partial w}{\partial y}\right)+A_{222}\frac{\partial^2\phi_\theta}{\partial y^2}\\&+F_{32}\frac{\partial\varphi}{\partial y}+A_{661}\left(\frac{\partial^2 u}{\partial y\,\partial x}+\frac{\partial^2 v}{\partial x^2}\right)+A_{662}\left(\frac{\partial^2\phi_x}{\partial y\,\partial x}+\frac{\partial^2\phi_y}{\partial x^2}\right)\end{aligned} \tag{83}$$

$$-k'A_{44}\left[\frac{\partial w}{\partial y}+\phi_y\right]-E_{15}\frac{\partial\varphi}{\partial y}=I_2\frac{\partial^2\phi_y}{\partial t^2}+I_1\frac{\partial^2 v}{\partial t^2},$$

$$\begin{aligned}\delta\phi: \;&-E_{15}\left(\frac{\partial\phi_x}{\partial x}+\frac{\partial^2 w}{\partial x^2}\right)+\Xi_{11}\left(\frac{\partial^2\varphi}{\partial x\,\partial y}\right)-E_{24}\left(\frac{\partial^2 w}{\partial y^2}+\frac{\partial\phi_y}{\partial y}\right)\\&+\Xi_{22}\left(\frac{\partial^2\varphi}{\partial y^2}\right)+E_{31}\frac{\partial u}{\partial x}+F_{31}\frac{\partial\phi_x}{\partial x}\\&+\frac{E_{32}}{R}\left(w+\frac{\partial v}{\partial y}\right)+F_{32}\frac{\partial\phi_y}{\partial y}-\Xi_{33}\varphi=0.\end{aligned} \tag{84}$$

where

$$\left(\Xi_{11},\Xi_{22}\right)=\int_{-h/2}^{h/2}\left(\in_{11},\in_{22}\right)\cos^2\left(\frac{\pi z}{h}\right)dz, \tag{85}$$

$$\left(\Xi_{33}\right)=\frac{\pi^2}{h^2}\int_{-h/2}^{h/2}\left(\in_{33}\right)\sin^2\left(\frac{\pi z}{h}\right)dz. \tag{86}$$

3. Solution procedure

Steady state solutions to the governing equations of the system motion and the electric potential distribution which relate to the simply supported boundary conditions and zero electric potential along the edges of the surface electrodes can be assumed as

$$u(x,y,t)=u_0\cos(\frac{n\pi x}{L})\sin(\frac{m\pi y}{b})e^{i\omega t}, \tag{87}$$

$$v(x,y,t)=v_0\sin(\frac{n\pi x}{L})\cos(\frac{m\pi y}{b})e^{i\omega t}, \tag{88}$$

$$w(x,y,t)=w_0\sin(\frac{n\pi x}{L})\sin(\frac{m\pi y}{b})e^{i\omega t}, \tag{89}$$

$$\phi_x(x,y,t)=\psi_{x0}\cos(\frac{n\pi x}{L})\sin(\frac{m\pi y}{b})e^{i\omega t}, \tag{90}$$

$$\phi_y(x,y,t)=\psi_{y0}\sin(\frac{n\pi x}{L})\cos(\frac{m\pi y}{b})e^{i\omega t}, \tag{91}$$

$$\varphi(x,y,t)=\varphi_0\sin(\frac{n\pi x}{L})\cos(\frac{m\pi y}{b})e^{i\omega t}, \tag{92}$$

Substituting Eqs. (87)-(92) into Eqs. (79)-(84) yields

$$\begin{bmatrix}K_{11}&K_{12}&K_{13}&K_{14}&K_{15}&K_{16}\\K_{21}&K_{22}&K_{23}&K_{24}&K_{25}&K_{26}\\K_{31}&K_{32}&K_{33}&K_{34}&K_{35}&K_{36}\\K_{41}&K_{42}&K_{43}&K_{44}&K_{45}&K_{46}\\K_{51}&K_{52}&K_{53}&K_{54}&K_{55}&K_{56}\\K_{61}&K_{62}&K_{63}&K_{64}&K_{65}&K_{66}\end{bmatrix}\begin{bmatrix}u_0\\v_0\\w_0\\\psi_{x0}\\\psi_{y0}\\\varphi_0\end{bmatrix}=0, \tag{93}$$

where K_{ij} are defined in Appendix A. Finally, for calculating

the frequency of the system (ω), the determinant of matrix in Eq. (93) should be equal to zero.

4. Numerical results and discussion

A computer program is prepared for the vibration smart control solution of concrete foundation reinforced with SiO_2 nanoparticles and piezoelectric layer. Here, poly vinilidene fluride (PVDF) is selected for the piezoelectric layer with the material properties of Table 1 (Kolahchi *et al*. 2016). In addition, SiO_2 nanoparticles have Yong's modulus of E_r = 70 GPa and Poisson's ratio of v_r = 0.2.

4.1 Validation

In this paper, to validate the results, the frequency of the structure is obtained by assuming the absence of soil medium (K_w = 0). Therefore, all the mechanical properties and type of loading are the same as Whitney (1987). So the non-dimensional frequency is considered as $\Omega = \sqrt{\frac{\rho h \omega^2 a^4}{D_0}}$ in which $D_0 = E_1 h^3 / (12\ (1 - v_{12}v_{21}))$. The results are compared with five references which have used different solution method. The exact solution is used by Whitney (1987) while discrete singular convolution approach is applied by Secgin and Sarigul (2008). The numerical solution method of Dai *et al*. (2004), Chen *et al*. (2003) and Chow *et al*. (1992) are mesh-free, finite element and Ritz, respectively. As it is observed in Table 2, the results of present work are in accordance with the mentioned references.

4.2 Effects of different parameters

Fig. 2 illustrates the effect of the SiO_2 nanoparticles volume fraction on the dimensionless frequency of structure

Table 1 Material properties of PVDF

Properties	PVDF
C_{11}	238.24 (GPa)
C_{12}	3.98 (GPa)
C_{22}	23.6 (GPa)
e_{11}	-0.135 (C/m^2)
e_{12}	-0.145 (C/m^2)
$\in_{11}$	1.1e-8 (C^2/Nm^2)

Table 2 Validation of present work with the other references

Method	Mode number			
	1	2	3	4
Whitney (1987)	15.171	33.248	44.387	60.682
Secgin and Sarigul (2008)	15.171	33.248	44.387	60.682
Dai *et al*. (2004)	15.17	33.32	44.51	60.78
Chen *et al*. (2003)	15.18	33.34	44.51	60.78
Chow *et al*. (1992)	15.19	33.31	44.52	60.79
Present	15.169	33.241	44.382	60.674

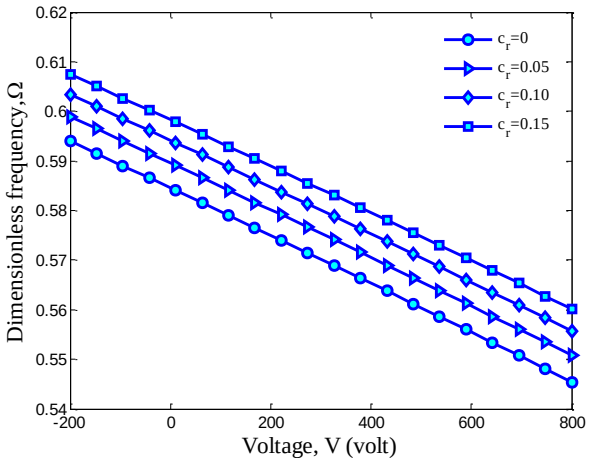

Fig. 2 Effects of SiO_2 nanoparticles volume percent on the dimension frequency versus dimension applied voltage external

$(\Omega = \omega L\sqrt{\rho_m / E_m})$. It can be seen that with increasing the values of SiO_2 nanoparticles volume fraction, the frequency of the system is increased. This is due to the fact that the increase of SiO_2 nanoparticles leads to a harder structure. However, it may be concluded that using nanotechnology for reinforce of concrete foundations has an important role in improving the vibration behavior of system.

Fig. 3 shows the effect of SiO_2 nanoparticles agglomeration on the dimensionless frequency of structure versus external applied voltage. As can be seen, considering agglomeration of SiO_2 nanoparticles leads to lower frequency. It is due to this point that the agglomeration of SiO_2 nanoparticles decreases the stability and homogeneity of the structure.

The dimensionless frequency of the nano-composite concrete foundation is demonstrated in Fig. 4 for different soil mediums. In this figure, four cases of loose sand, dense sand, Clayey medium dense sand and Clayey soil are considered with the spring constants of Table 3. As can be seen, considering soil medium increases the frequency of the structure. It is due to the fact that considering soil

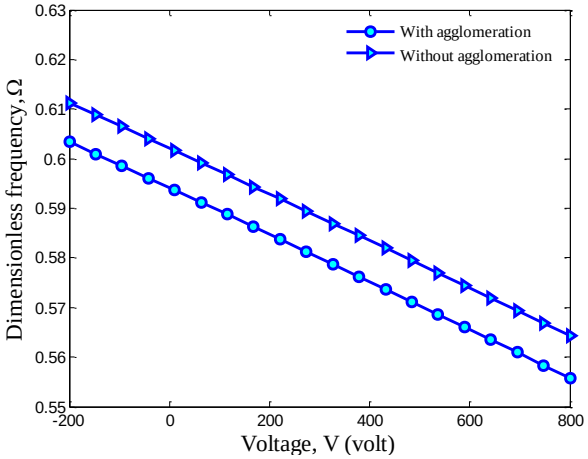

Fig. 3 Effects of SiO_2 nanoparticles agglomeration on the dimension frequency versus dimension external applied voltage

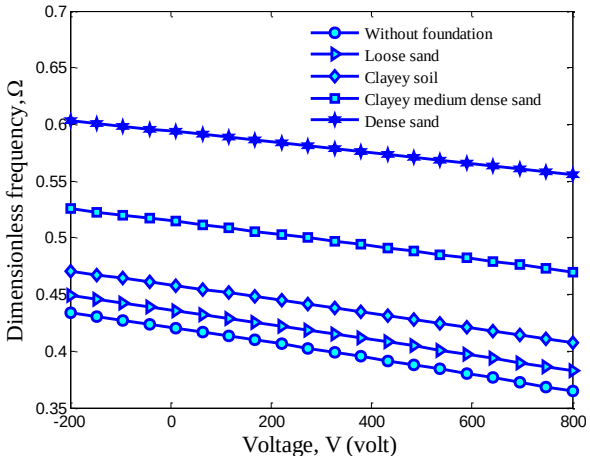

Fig. 4 Effects of soil medium on the dimension frequency versus dimension external applied voltage

Table 3 Spring constants of soil mediums under concrete foundation

Soil	K_w (N/m^3)
Loose sand	4800-16000
Dense sand	64000-128000
Clayey medium dense sand	32000-80000
Clayey soil	12000-24000

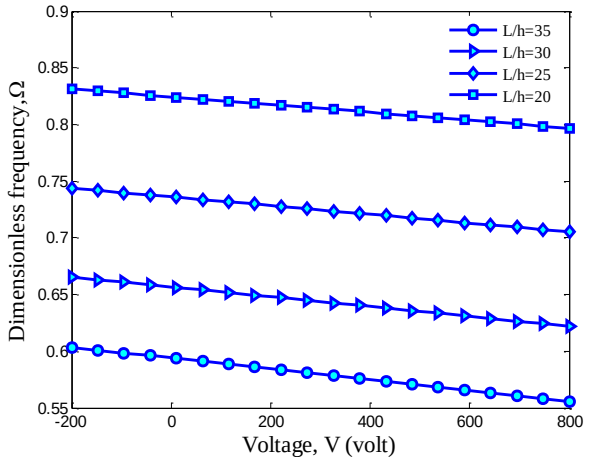

Fig. 5 Effects of length to thickness ratio of concrete foundation on the dimension frequency versus dimension external applied voltage

medium leads to stiffer structure. Furthermore, the frequency of the dense sand medium is higher than other cases since the spring constant of this medium is maximum.

The effect of the length to thickness ratio of concrete foundation on the dimensionless frequency of the system is depicted in Fig. 5. As can be seen, the frequency of the structure decreases with increasing the length to thickness ratio. It is because increasing the length to thickness ratio leads to softer structure.

Fig. 6 shows the dimensionless frequency of the structure for different length to width ratio of the concrete

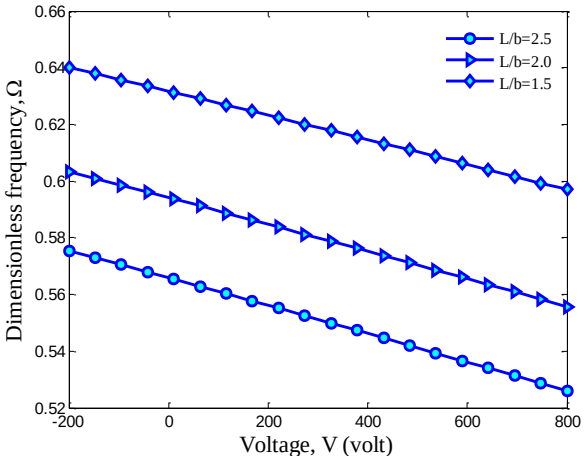

Fig. 6 Effects of length to width ratio of concrete foundation on the dimension frequency versus dimension external applied voltage

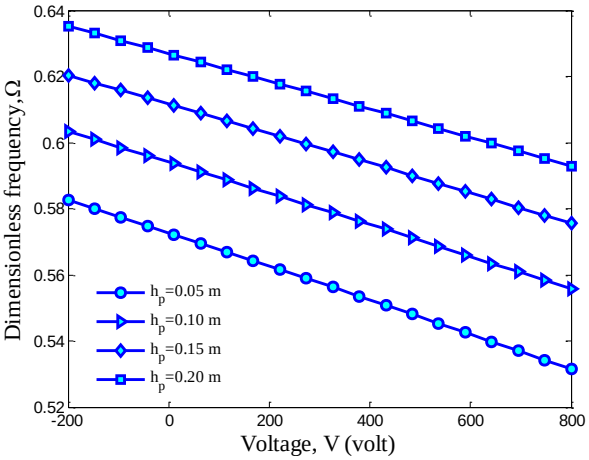

Fig. 7 Effects of piezoelectric layer thickness on the dimension frequency versus dimension external applied voltage

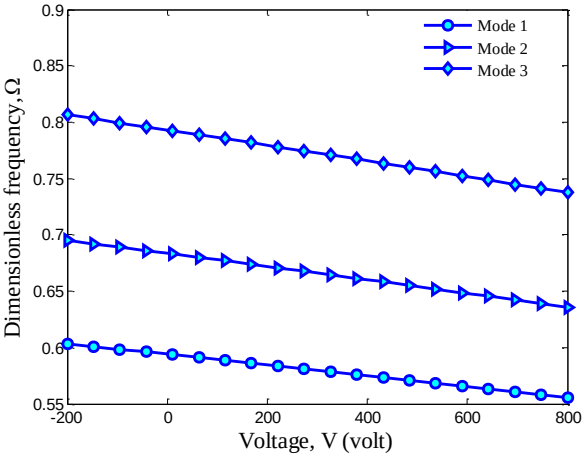

Fig. 8 Effects of mode number on the dimension frequency versus dimension external applied voltage

foundation. It can be also found that the frequency of the structure decrease with increasing the length to width ratio

which is due to the higher stiffness of system with lower length to width ratio.

The effect of piezoelectric layer thickness on the dimensionless frequency is shown in Fig. 7. It can be found that with increasing the piezoelectric layer thickness, the frequency of the structure is increased. It is because with increasing the piezoelectric layer thickness, the stiffness of the structure will be improved.

The effect of mode numbers on the dimensionless frequency of system against external applied voltage is plotted in Fig. 8. As can be seen, with increasing the mode numbers, the frequency increases.

5. Conclusions

Vibration smart control of embedded concrete foundations reinforced with SiO_2 nanoparticles and covered with a piezoelectric layer subjected to external voltage was the main contribution of the present paper. Mori-Tanaka model is used for obtaining the effective material properties of the structure considering agglomeration effects. The soil medium was simulated by Winkler foundation. Based on orthotropic FSDT, the motion equations were derived using energy method and Hamilton's principle. Exact solution is applied for obtaining the frequency of system so that the effects of the applied voltage, volume percent and agglomeration of SiO_2 nanoparticles, soil medium and geometrical parameters of concrete foundation were considered. It can be seen that with increasing the values of SiO_2 nanoparticles volume fraction, the frequency of the system was increased. Considering agglomeration of SiO_2 nanoparticles leads to lower frequency. It can be seen that considering soil medium increases the frequency of the structure. Furthermore, the frequency of the dense sand medium was higher than other cases since the spring constant of this medium was maximum. In addition, the frequency of the structure decreases with increasing the length to thickness ratio and length to width ratio of the concrete foundation. It can be found that with increasing the piezoelectric layer thickness, the frequency of the structure was increased. Present results are in good agreement with those reported by the other references. Finally, it is hoped that the results presented in this paper would be helpful for control and design of concrete foundations.

References

Ahouel, M., Houari, M.S.A., Adda Bedia, E.A. and Tounsi, A. (2016), "Size-dependent mechanical behavior of functionally graded trigonometric shear deformable nanobeams including neutral surface position concept", *Steel Compos. Struct., Int. J.*, **20**(5), 963-981.

Akgoz, B. and Civalek, O. (2011), "Nonlinear vibration analysis of laminated plates resting on nonlinear two-parameters elastic foundations", *Steel Compos. Struct., Int. J.*, **11**(5), 403-421.

Alibeigloo, A. (2013), "Static analysis of functionally graded carbon nanotube-reinforced composite plate embedded in piezoelectric layers by using theory of elasticity", *Compos. Struct.*, **95**, 612-622.

Arbabi, A., Kolahchi, R. and Rabani Bidgoli, M. (2017), "Concrete columns reinforced with Zinc Oxide nanoparticles subjected to electric field: Buckling analysis", *Wind Struct., Int. J.*, **24**(5), 431-446.

Attia, A., Tounsi, A., Adda Bedia, E.A. and Mahmoud, S.R. (2015), "Free vibration analysis of functionally graded plates with temperature-dependent properties using various four variable refined plate theories", *Steel Compos. Struct., Int. J.*, **18**(1), 187-212.

Bahmyari, E. and Khedmati, M.R. (2013), "Vibration analysis of nonhomogeneous moderately thick plates with point supports resting on Pasternak elastic foundation using element free Galerkin method", *Eng. Anal. Bound. Elem.*, **37**(10), 1212-1238.

Belabed, Z., Houari, M.S.A., Tounsi, A., Mahmoud, S.R. and Bég, O.A. (2014), "An efficient and simple higher order shear and normal deformation theory for functionally graded material (FGM) plates", *Compos.: Part B*, **60**, 274-283.

Beldjelili, Y., Tounsi, A. and Mahmoud, S.R. (2016), "Hygro-thermo-mechanical bending of S-FGM plates resting on variable elastic foundations using a four-variable trigonometric plate theory", *Smart Struct. Syst., Int. J.*, **18**(4), 755-786.

Belkorissat, I., Houari, M.S.A., Tounsi, A. and Hassan, S. (2015), "On vibration properties of functionally graded nano-plate using a new nonlocal refined four variable model", *Steel Compos. Struct., Int. J.*, **18**(4), 1063-1081.

Bellifa, H., Benrahou, K.H., Hadji, L., Houari, M.S.A. and Tounsi, A. (2016), "Bending and free vibration analysis of functionally graded plates using a simple shear deformation theory and the concept the neutral surface position", *J Braz. Soc. Mech. Sci. Eng.*, **38**(1), 265-275.

Bellifa, H., Benrahou, K.H., Bousahla, A.A., Tounsi, A. and Mahmoud, S.R. (2017), "A nonlocal zeroth-order shear deformation theory for nonlinear postbuckling of nanobeams", *Struct. Eng. Mech., Int. J.*, **62**(6), 695 - 702.

Bennoun, M., Houari, M.S.A. and Tounsi, A. (2016), "A novel five variable refined plate theory for vibration analysis of functionally graded sandwich plates", *Mech. Advan. Mat. Struct.*, **23**(4), 423-431.

Bessaim, A., Houari, M.S.A. and Tounsi, A. (2013), "A new higher-order shear and normal deformation theory for the static and free vibration analysis of sandwich plates with functionally graded isotropic face sheets", *J. Sandw. Struct. Mater.*, **15**(6), 671-703.

Besseghier, A., Houari, M.S.A., Tounsi, A. and Hassan, S. (2017), "Free vibration analysis of embedded nanosize FG plates using a new nonlocal trigonometric shear deformation theory", *Smart Struct. Syst., Int. J.*, **19**(6), 601-614.

Bouafia, Kh., Kaci, A., Houari M.S.A. and Tounsi, A. (2017), "A nonlocal quasi-3D theory for bending and free flexural vibration behaviors of functionally graded nanobeams", *Smart Struct. Syst., Int. J.*, **19**(2), 115-126.

Bouderba, B., Houari, M.S.A. and Tounsi, A. (2013), "Thermo-mechanical bending response of FGM thick plates resting on Winkler–Pasternak elastic foundations", *Steel Compos. Struct., Int. J.*, **14**(1), 85-104.

Bouderba, B., Houari, M.S.A., Tounsi, A. and Mahmoud, S.R. (2016), "Thermal stability of functionally graded sandwich plates using a simple shear deformation theory", *Struct. Eng. Mech., Int. J.*, **58**(3), 397-422.

Boukhari, A., Atmane, H.A., Tounsi, A., Adda Bedia, E.A. and Mahmoud, S.R. (2016), "An efficient shear deformation theory for wave propagation of functionally graded material plates", *Struct. Eng. Mech., Int. J.*, **57**(5), 837-859.

Bounouara, F., Benrahou, K.H., Belkorissat, I. and Tounsi A. (2016), "A nonlocal zeroth-order shear deformation theory for free vibration of functionally graded nanoscale plates resting on elastic foundation", *Steel Compos. Struct., Int. J.*, **20**(2), 227-

249.

Bourada, M., Kaci, A., Houari, M.S.A. and Tounsi, A. (2015), "A new simple shear and normal deformations theory for functionally graded beams", *Steel Compos. Struct., Int. J.*, **18**(2), 409-423.

Bousahla, A.A., Benyoucef, S., Tounsi, A. and Mahmoud, S.R. (2016), "On thermal stability of plates with functionally graded coefficient of thermal expansion", *Struct. Eng. Mech., Int. J.*, **60**(2), 313-335.

Chikh, A., Tounsi, A., Hebali, H. and Mahmoud, S.R. (2017), "Thermal buckling analysis of cross-ply laminated plates using a simplified HSDT", *Smart Struct. Syst., Int. J.*, **19**(3), 289-297.

Bowles, J.E. (1988), *Foundation Analysis and Design*, McGraw Hill Inc.

Buczkowski, R. and Torbacki, W. (2001), "Finite element modelling of thick plates on two-parameter elastic foundation", *Int. J. Numer. Anal. Met.*, **25**(14), 1409-1427.

Chen, X.L., Liu, G.R. and Lim, S.P. (2003), "An element free Galerkin method for the free vibration analysis of composite laminates of complicated shape", *Compos. Struct.*, **59**(2), 279-289.

Chen, J., Li, P., Song, G. and Ren, Z. (2016a), "Piezo-based wireless sensor network for early-age concrete strength monitoring", *Optik*, **127**(5), 2983-2987.

Chen, S.S., Liao, K.H. and Shi, J.Y. (2016b), "A dimensionless parametric study for forced vibrations of foundation-soil systems", *Comput. Geotech.*, **76**, 184-193.

Chow, S.T., Liew, K.M. and Lam, K.Y. (1992), "Transverse vibration of symmetrically laminated rectangular composite plates", *Compos. Struct.*, **20**(4), 213-226.

Dai, K.Y., Liu, G.R., Lim, M.K. and Chen, X.L. (2004), "A mesh-free method for static and free vibration analysis of shear deformable laminated composite plates", *J. Sound Vib.*, **269**(3-5), 633-652.

De Rosa, M.A. and Lippiello, M. (2009), "Free vibrations of simply supported double plate on two models of elastic soils", *Int. J. Numer. Anal. Methods Geomech.*, **33**(3), 331-353.

Draiche, K., Tounsi, A. and Mahmoud, S.R. (2016), "A refined theory with stretching effect for the flexure analysis of laminated composite plates", *Geomech. Eng., Int. J.*, **11**(5), 671-690.

Duc, N.D., Hadavinia, H., Van Thu, P. and Quan, T.Q. (2015), "Vibration and nonlinear dynamic response of imperfect three-phase polymer nanocomposite panel resting on elastic foundations under hydrodynamic loads", *Compos. Struct.*, **131**, 229-237.

Duc, N.D., Cong, P.H., Tuan, N.D., Tran, P. and Van Thanh, N. (2017a), "Thermal and mechanical stability of functionally graded carbon nanotubes (FG CNT)-reinforced composite truncated conical shells surrounded by the elastic foundation", *Thin-Wall. Struct.*, **115**, 300-310.

Duc, N.D., Lee, J., Nguyen-Thoi, T. and Thang, P.T. (2017b), "Static response and free vibration of functionally graded carbon nanotube-reinforced composite rectangular plates resting on Winkler–Pasternak elastic foundations", *Aerosp. Sci. Technol.*, **68**, 391-402.

Duc, N.D., Tran, Q.Q. and Nguyen, D.K. (2017c), "New approach to investigate nonlinear dynamic response and vibration of imperfect functionally graded carbon nanotube reinforced composite double curved shallow shells subjected to blast load and temperature", *Aerosp. Sci. Technol.*, **71**, 360-372.

Duc, N.D., Seung-Eock, K., Quan, T.Q., Long, D.D. and Anh, V.M. (2018), "Nonlinear dynamic response and vibration of nanocomposite multilayer organic solar cell", *Compos. Struct.*, **184**, 1137-1144.

Ebrahimi, F., Jafari, A. and Barati, M.R. (2017), "Vibration analysis of magneto-electro-elastic heterogeneous porous material plates resting on elastic foundations", *Thin-Wall. Struct.*, **119**, 33-46.

El-Haina, F., Bakora, A., Bousahla, A.A. and Hassan, S. (2017), "A simple analytical approach for thermal buckling of thick functionally graded sandwich plates", *Struct. Eng. Mech., Int. J.*, **63**(5), 585-595.

Fathi, M., Yousefipour, A. and Hematpoury Farokhy, E. (2017), "Mechanical and physical properties of expanded polystyrene structural concretes containing Micro-silica and Nano-silica", *Constr. Build. Mater.*, **136**, 590-597.

Ferreira, A.J.M., Roque, C.M.C., Neves, A.M.A., Jorge, R.M.N. and Soares, C.M.M. (2010), "Analysis of plates on Pasternak foundations by radial basis functions", *Comput. Mecch.*, **46**(6), 791-803.

Henderson, J.P., Plummer, A. and Johnston, N. (2018), "An electro-hydrostatic actuator for hybrid active-passive vibration isolation", *Int. J. Hydromechatronics*, **1**, 47-71.

Jafarian Arani, A. and Kolahchi, R. (2016), "Buckling Analysis of embedded concrete columns armed with carbon nanotubes", *Comput. Concrete, Int. J.*, **17**(5), 567-578.

Kolahchi, R., Hosseini, H. and Esmailpour, M. (2016), "Differential cubature and quadrature-Bolotin methods for dynamic stability of embedded piezoelectric nanoplates based on visco-nonlocal-peizoelasticity theories", *Compos. Struct.*, **157**, 174-186.

Khetir, H., Bouiadjra, M.B., Houari, M.S.A., Tounsi, A. and Mahmoud, S.R. (2017), "A new nonlocal trigonometric shear deformation theory for thermal buckling analysis of embedded nanosize FG plates", *Struct. Eng. Mech., Int. J.*, **64**(4), 391-402.

Kumar, Y. and Lal, R. (2012), "Vibrations of nonhomogeneous orthotropic rectangular plates with bilinear thickness variation resting on Winkler foundation", *Meccanica*, **47**(4), 893-915.

Lam, K.Y, Wang, C.M. and He, X.Q. (2000), "Canonical exact solutions for levy-plates on two-parameter foundation using green's functions", *Eng. Struct.*, **22**(4), 364-378.

Larbi Chaht, F., Kaci, A., Houari, M.S.A. and Hassan, S. (2015), "Bending and buckling analyses of functionally graded material (FGM) size-dependent nanoscale beams including the thickness stretching effect" *Steel Compos. Struct., Int. J.*, **18**(2), 425-442.

Li, Y. and Zhang, J. (2014), "Free vibration analysis of magnetoelectroelastic plate resting on a Pasternak foundation", *Smart Mater. Struct.*, **23**(2), 025002.

Mahi, A., Bedia, E.A.A. and Tounsi, A. (2015), "A new hyperbolic shear deformation theory for bending and free vibration analysis of isotropic, functionally graded, sandwich and laminated composite plates", *Appl. Math. Model.*, **39**(9), 2489-2508.

Mantari, J.L. and Granados, E.V. (2016), "An original FSDT to study advanced composites on elastic foundation", *Thin-Wall. Struct.*, **107**, 80-89.

Mantari, J.L., Granados, E.V. and Guedes Soares, C. (2014), "Vibrational analysis of advanced composite plates resting on elastic foundation", *Compos. Part B-Eng.*, **66**, 407-419.

Meftah, A., Bakora, A., Zaoui, F.Z., Tounsi A. and Adda Bedia E.A. (2017), "A non-polynomial four variable refined plate theory for free vibration of functionally graded thick rectangular plates on elastic foundation", *Steel Compos. Struct., Int. J.*, **23**(3), 317-330.

Mehri, M., Asadi, H. and Wang, Q. (2016), "Buckling and vibration analysis of a pressurized CNT reinforced functionally graded truncated conical shell under an axial compression using HDQ method", *Comput. Meth. Appl. Mech. Eng.*, **303**, 75-100.

Menasria, A., Bouhadra, A., Tounsi, A. and Hassan, S. (2017), "A new and simple HSDT for thermal stability analysis of FG sandwich plates", *Steel Compos. Struct., Int. J.*, **25**(2), 157-175.

Meziane, M.A.A., Abdelaziz, H.H. and Tounsi, A.T. (2014), "An efficient and simple refined theory for buckling and free vibration of exponentially graded sandwich plates under various

boundary conditions", *J. Sandw. Struct. Mater.*, **16**(3), 293-318.
Mori, T. and Tanaka, K. (1973), "Average stress in matrix and average elastic energy of materials with misfitting inclusions", *Acta Metall. Mater.*, **21**(5), 571-574.
Mouffoki, A., Adda Bedia, E.A., Houari M.S.A. and Hassan, S. (2017), "Vibration analysis of nonlocal advanced nanobeams in hygro-thermal environment using a new two-unknown trigonometric shear deformation beam theory", *Smart Struct. Syst., Int. J.*, **20**(3), 369-383.
Nirmala, J. and Dhanalakshmi, G. (2015), "Influence of nano materials in the distressed retaining structure for crack filling", *Constr. Build. Mater.*, **88**, 225-231.
Persson, P., Persson, K. and Sandberg, G. (2016), "Numerical study on reducing building vibrations by foundation improvement", *Eng. Struct.*, **124**, 361-375.
Reddy, J.N. (2002), *Mechanics of Laminated Composite Plates and Shells*: *Theory and Analysis*, (2nd Edition), CRC Press.
Sanada, K. (2018), "Real-time implementation of Kalman filter for unsteady flow measurement in a pipe", *Int. J. Hydromechatronics*, **1**, 3-15.
Sasmal, S., Ravivarman, N., Sindu, B.S. and Vignesh, K. (2017), "Electrical conductivity and piezo-resistive characteristics of CNT and CNF incorporated cementitious nanocomposites under static and dynamic loading", *Compos. Part A-Appl. S.*, **100**, 227-243.
Secgin, A. and Sarigul, A.S. (2008), "Free vibration analysis of symmetrically laminated thin composite plates by using discrete singular convolution (DSC) approach: Algorithm and verification", *J. Sound Vib.*, **315**(1-2), 197-211.
Shi, D.L. and Feng, X.Q. (2004), "The Effect of nanotube waviness and agglomeration on the elastic property of carbon nanotube-reinforced composites", *J. Eng. Mater-T. ASME*, **126**(3), 250-270.
Shooshtari, A. and Razavi, S. (2015), "Large amplitude free vibration of symmetrically laminated magneto-electro-elastic rectangular plates on Pasternak type foundation", *Mech. Res. Commun.*, **69**, 103-113.
Stelson, K.A. (2018), "Academic fluid power research in the USA", *Int. J. Hydromechatronics*, **1**, 126-152.
Su, Y., Li, J., Wu, C., Wu, P. and Li, Z.X. (2016), "Influences of nano-particles on dynamic strength of ultra-high performance concrete", *Compos. Part B-Eng.*, **91**, 595-609.
Thanh, N.V., Khoa, N.D., Tuan, N.D., Tran, P. and Duc, N.D. (2017), "Nonlinear dynamic response and vibration of functionally graded carbon nanotube-reinforced composite (FG-CNTRC) shear deformable plates with temperature-dependent material properties", *J. Therm. Stres.*, **40**(10), 1254-1274.
Uğurlu, B. (2016), "Boundary element method based vibration analysis of elastic bottom plates of fluid storage tanks resting on Pasternak foundation", *Eng. Anal. Bound. Elem.*, **62**, 163-176.
Van Thu, P. and Duc, N.D. (2016), "Non-linear dynamic response and vibration of an imperfect three-phase laminated nanocomposite cylindrical panel resting on elastic foundations in thermal environment", *Sci. Eng. Compos. Mat.*, **24**(6), 951-962.
Whitney, J.M. (1987), *Structural Analysis of Laminated Anisotropic Plates*, Technomic Publishing Company Inc., PA, USA.
Xue, C.X., Pan, E., Zhang, S.Y. and Chu, H.J. (2011), "Large deflection of a rectangular magnetoelectroelastic thin plate", *Mech. Res. Commun.*, **38**(7), 518-523.
Zamanian, M., Kolahchi, R. and Rabani Bidgoli, M. (2017), "Agglomeration effects on the buckling behavior of embedded concrete columns reinforced with SiO_2 nanoparticles", *Wind Struct., Int. J.*, **24**(1), 43-57.
Zemri, A., Houari, M.S.A., Bousahla, A.A. and Tounsi A. (2015), "A mechanical response of functionally graded nanoscale beam: an assessment of a refined nonlocal shear deformation theory beam theory", *Struct. Eng. Mech., Int. J.*, **54**(4), 693-710.
Zhou, D., Cheung, Y.K., Lo, S.H. and Au, F.T.K. (2004), "Three-dimensional vibration analysis of rectangular thick plates on Pasternak foundation", *Int. J. Numer. Meth. Eng.*, **59**(10), 1313-1334.
Zidi, M., Tounsi, A. and Bég, O.A. (2014), "Bending analysis of FGM plates under hygro-thermo-mechanical loading using a four variable refined plate theory", *Aerosp. Sci. Tech.*, **34**, 24-34.

CC

Appendix A

$$K_{11} = -\frac{A_{110}n^2\pi^2}{L^2} - \frac{A_{660}m^2\pi^2}{b^2} + I_0\omega^2, \tag{A1}$$

$$K_{12} = -\frac{A_{120}nm\pi^2}{bL} - \frac{A_{660}nm\pi^2}{bL}, \tag{A2}$$

$$K_{13} = 0, \tag{A3}$$

$$K_{14} = -\frac{A_{661}m^2\pi^2}{b^2} - \frac{A_{111}n^2\pi^2}{L^2} + I_2\omega^2, \tag{A4}$$

$$K_{15} = -\frac{A_{661}mn\pi^2}{bL} - \frac{A_{121}mn\pi^2}{bL}, \tag{A5}$$

$$K_{16} = 0, \tag{A6}$$

$$K_{21} = -\frac{A_{120}nm\pi^2}{bL} - \frac{A_{660}nm\pi^2}{bL}, \tag{A7}$$

$$K_{22} = -\frac{A_{220}m^2\pi^2}{b^2} - \frac{A_{660}n^2\pi^2}{L^2} + I_0\omega^2, \tag{A8}$$

$$K_{23} = 0, \tag{A9}$$

$$K_{24} = -\frac{A_{661}mn\pi^2}{bL} - \frac{A_{121}mn\pi^2}{bL}, \tag{A10}$$

$$K_{25} = -\frac{A_{221}m^2\pi^2}{R^2} - \frac{A_{661}n^2\pi^2}{L^2} + I_2\omega^2, \tag{A11}$$

$$K_{26} = 0, \tag{A12}$$

$$K_{31} = \frac{A_{121}nm\pi^2}{bL}, \tag{A13}$$

$$K_{32} = \frac{A_{22}m^2\pi^2}{b^2}, \tag{A14}$$

$$\begin{aligned} K_{33} = -K_w &- \frac{k'A_{55}n^2\pi^2}{L^2} - \frac{k'A_{44}m^2\pi^2}{b^2} \\ &- 2V_0e_{31}\frac{n^2\pi^2}{L^2} - 2V_0e_{32}\frac{n^2\pi^2}{b^2} + I_0\omega^2, \end{aligned} \tag{A15}$$

$$K_{34} = -\frac{k'A_{55}n\pi}{L} + \frac{A_{121}nm\pi^2}{bL}, \tag{A16}$$

$$K_{35} = -\frac{k'A_{44}m\pi}{b} + \frac{A_{221}mn\pi^2}{bL}, \tag{A17}$$

$$K_{36} = \frac{E_{24}n^2\pi^2}{L^2} + \frac{E_{15}m^2\pi^2}{b^2}, \tag{A18}$$

$$K_{41} = -\frac{A_{661}m^2\pi^2}{b^2} - \frac{A_{111}n^2\pi^2}{L^2} + I_2\omega^2, \tag{A19}$$

$$K_{42} = -\frac{A_{661}mn\pi^2}{bL} - \frac{A_{121}mn\pi^2}{bL}, \tag{A20}$$

$$K_{43} = -\frac{k'A_{55}n\pi}{L}, \tag{A21}$$

$$K_{44} = -\frac{A_{111}n^2\pi^2}{L^2} - \frac{A_{661}m^2\pi^2}{b^2} - k'A_{55} + I_3\omega^2, \tag{A22}$$

$$K_{45} = -\frac{A_{122}nm\pi^2}{Lb} - \frac{A_{662}nm\pi^2}{bL}, \tag{A23}$$

$$K_{46} = \frac{E_{31}n}{L} + \frac{E_{24}n}{L}, \tag{A24}$$

$$K_{51} = -\frac{A_{661}mn\pi^2}{bL} - \frac{A_{121}mn\pi^2}{bL}, \tag{A25}$$

$$K_{52} = -\frac{A_{221}m^2\pi^2}{b^2} - \frac{A_{661}n^2\pi^2}{L^2} + I_2\omega^2, \tag{A26}$$

$$K_{53} = -\frac{k'A_{44}m\pi}{b}, \tag{A27}$$

$$K_{54} = -\frac{A_{122}nm\pi^2}{Lb} - \frac{A_{662}nm\pi^2}{bL}, \tag{A28}$$

$$K_{55} = -\frac{A_{662}n^2\pi^2}{L^2} - \frac{A_{222}m^2\pi^2}{b^2} - k'A_{44} + I_3\omega^2, \tag{A29}$$

$$K_{56} = \frac{E_{32}m}{b} + \frac{E_{15}m}{b}, \tag{A30}$$

$$K_{61} = 0, \tag{A31}$$

$$K_{62} = 0, \tag{A32}$$

$$K_{63} = +\frac{E_{24}m^2\pi^2}{b^2} + \frac{E_{15}n^2\pi^2}{L^2}, \tag{A33}$$

$$K_{64} = \frac{E_{24}n}{L}, \tag{A34}$$

$$K_{56} = \frac{E_{24}m}{b}, \tag{A35}$$

$$K_{66} = \frac{\Xi_{11}n^2\pi^2}{L^2} + \frac{\Xi_{22}m^2\pi^2}{b^2} + \Xi_{33}\pi^2. \tag{A36}$$